Intensity and pressure dependence of resonance fluorescence of OH induced by a tunable uv laser

D. K. Killinger,* Charles C. Wang,† and M. Hanabusa†
Scientific Research Staff, Ford Motor Company, Dearborn, Michigan 48121
(Received 2 February 1976)

We have investigated the intensity and pressure dependence of the fluorescence spectrum of OH in the presence of N_2 and H_2O molecules. Saturation of the absorption transition was observed at low pressures, and the corresponding fluorescence signal was found to vary as the square root of the exciting intensity. This observed dependence agreed with the predicted dependence which took into account the presence of laser modes in the spectrum of the exciting radiation. With full laser power incident, a saturation parameter as high as 3×10^5 was observed. The fluorescence spectrum was found to peak at 3145 Å and at 3090 Å, with the relative peak intensities dependent upon gas pressures and upon the particular rotational electronic transition used for excitation. It is concluded that vibrational relaxation of the electronically excited OH due to water vapor in the system plays a dominant role in determining the observed fluorescence spectrum.

I. INTRODUCTION

In recent years, the technique of laser-induced fluorescence has been employed for the measurement of hydroxyl (OH) concentrations in ambient air[1] and in flames.[2] This technique involves exciting the OH radicals using one of the rotational electronic lines in the $^2\Pi(v''=0) \rightarrow {}^2\Sigma^+(v'=1)$ transitions and observing the fluorescence emission associated with the $^2\Sigma^+(v'=1) \rightarrow {}^2\Pi(v''=1)$ transitions near 3145 Å and the $^2\Sigma^+(v'=0) \rightarrow {}^2\Pi(v''=0)$ transitions near 3090 Å (Fig. 1). Because of the availability of high-power laser sources and the occurrence of fluorescence sufficiently red shifted from the exciting radiation, this technique has proved to be unprecedented in both sensitivity and selectivity.

It has been noted[3] that saturation of the absorption transition may set in at high exciting intensities, and that the observed fluorescence spectrum[1,2] is determined by the extent of cross relaxation of the excited OH before it fluoresces, but details of the relaxation processes were not established. This paper reports some experimental studies aimed at elucidating these relaxation processes which determine the intensity and the spectrum of the fluorescence signal under nitrogen atmosphere. These studies are important since they must be taken into account in the detection of OH at high altitudes in the atmosphere.[4]

Results of our studies indicate that the fluorescence signal of OH varied as the square root of the exciting laser intensity at low pressures. This dependence is to be expected when the absorption line is inhomogeneously broadened and there are discrete modes present in the spectrum of the exciting laser beam. Our results also indicate that both cross (rotational and vibrational) relaxation due to nitrogen molecules and direct vibrational relaxation by water and nitrogen molecules are important for the electronically excited OH.

In Sec. II, a brief account will be given of the saturation of the absorption transitions with different types of line broadening, and of the expected fluorescence spectrum. It is demonstrated there that the presence of laser modes in the spectrum of the exciting radiation is important in determining the effective rate of absorption. Application of this general consideration to OH is also indicated there. The experimental details are presented in Sec. III and the results are discussed in Sec. IV.

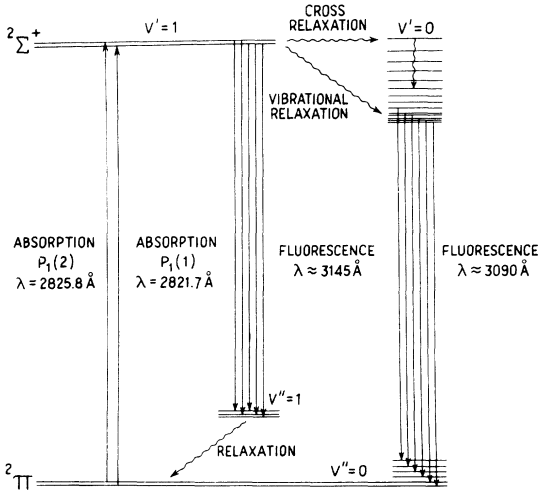

FIG 1. Schematic of OH levels involved in laser-induced fluorescence.

II. THEORETICAL BACKGROUND

A. Resonant absorption of radiation

In this section a brief account will be given of the absorption process of a molecule in the presence of a radiation field in resonance with the absorption transition. At low intensities, the steady-state rate of absorption varies linearly with the intensity of excitation: At high intensities, however, saturation[5] sets in and the rate of absorption deviates from this linear dependence in a way which depends both upon the nature of the line broadening and upon the spectral content of the exciting radiation. To be covered below are those cases which will be relevant to our subsequent discussions on OH absorption transitions.

1. Homogeneously broadened absorption transition induced by single-frequency radiation. The rate of absorption γ_{ab} due to single-frequency excitation is given by[3,5,6]

$$\gamma_{ab} = N_1 \sigma_0 F g(\nu_a, S_a). \tag{1}$$

Here N_1 is the concentration of the molecules that partake in the absorption transition, σ_0 is the integrated absorption cross section for the transition, F is the photon flux (photons/cm^2 sec) at the incident frequency ν_l, and

$$g(\nu_a, S_a) = \frac{1}{\pi} \frac{\frac{1}{2}\Delta\nu_0}{(\nu_l - \nu_a)^2 + (\frac{1}{2}\Delta\nu_0)^2(1+S_a)} \tag{2}$$

is the saturation-broadened line-shape function associated with a resonant transition with center frequency ν_a. In Eq. (2), $\Delta\nu_0$ is the homogeneous line width [full width at half-maximum (FWHM)] of the transition at zero intensity, and

$$S_a = 2\tau\sigma_0(2/\pi\Delta\nu_0)F \tag{3}$$

is the saturation parameter, with τ being the characteristic relaxation time associated with the transition. When the incident radiation is on-resonance with the absorption transition, Eq. (1) reduces to the following expression:

$$\gamma_{ab} = N_1\sigma_0 F(2/\pi\Delta\nu_0)(1+S_a)^{-1}. \tag{4}$$

One notes from Eqs. (3) and (4) that $S_a \to 0$ in the limit of zero intensity and the corresponding rate of absorption increases linearly with the intensity of excitation. In the limit of high intensity, however, the rate of absorption approaches a constant value independent of the intensity of excitation.

2. Inhomogeneously broadened absorption transition induced by single-frequency radiation. In the case of an inhomogeneously broadened transition, Eq. (1) should be modified to take into account the distributed nature of the oscillators responsible for the absorption, as follows:

$$\gamma_{ab} = N_1\sigma_0 F \int_{-\infty}^{+\infty} d\nu_a\, p(\nu_a) g(\nu_a, S_a), \tag{5}$$

where

$$\int_{-\infty}^{+\infty} d\nu_a\, p(\nu_a) = 1, \tag{6}$$

$$p(\nu_a) = \left(\frac{4\ln 2}{\pi}\right)^{1/2} \Delta\nu_D^{-1} \exp\left(\frac{-4(\ln 2)(\nu_a - \nu_D)^2}{\Delta\nu_D^2}\right), \tag{7}$$

for a Gaussian distribution with center frequency ν_D and a Doppler-broadened linewidth (FWHM) of $\Delta\nu_D$. In the limit $\Delta\nu_0 \ll \Delta\nu_D$ and with the incident radiation on-resonance with ν_D, Eq. (5) can be integrated to give

$$\gamma_{ab} = N_1\sigma_0 F[4(\ln 2)/\pi]^{1/2}\Delta\nu_D^{-1}(1+S_a)^{-1/2}. \tag{8}$$

At high intensities, the homogeneously power-broadened linewidth $\Delta\nu_0(1+S_a)^{1/2}$ may become comparable to the inhomogeneously broadened linewidth $\Delta\nu_D$. In this limit, Eq. (8) is no longer valid and the absorption rate approaches the high-intensity limit described previously for Eq. (4).

3. Absorption transition induced by an exciting radiation with uniform spectral distribution. When the exciting radiation is spread uniformly over a spectral width of $\Delta\nu_l$, the absorption rate for a homogeneously broadened line is given by

$$\gamma_{ab} = N_1\sigma_0 P/(1 + 2\tau\sigma_0 P), \tag{9}$$

where

$$P = \int_{-\infty}^{\infty} d\nu_l\, F(\nu_l) g(\nu_l, 0), \tag{10}$$

and $F \approx F(\nu_l)\Delta\nu_l$ is the total intensity of excitation. Equation (9) is similar to Eq. (1) with the exception that the total rate of absorption is integrated over the width of the intensity distribution. In the limit $\Delta\nu_l \gg \Delta\nu_0$, Eq. (9) integrates to give

$$\gamma_{ab} = N_1\sigma_0(F/\Delta\nu_l)(1+S_c)^{-1}, \tag{11}$$

where

$$S_c = 2\tau\sigma_0(F/\Delta\nu_l) \tag{12}$$

may be likened to the saturation parameter defined previously.

Equation (11) is also expected to be valid for an inhomogeneously broadened line with $\Delta\nu_l \gg \Delta\nu_D \gg \Delta\nu_0$. One notes from Eq. (11) that the rate of absorption saturates in a manner similar to that depicted in Eq. (4) for a homogeneously broadened line interacting with a single-frequency excitation.

4. Inhomogeneously broadened transition induced by radiation with discrete spectral components (or modes). We consider finally the case when the exciting radiation exhibits discrete fre-

quency components (or modes) rather than a uniform intensity distribution over the entire spectral width $\Delta\nu_l$. This case is of practical importance, since the output from a tunable dye laser used for excitation is most likely to contain a number of cavity modes rather than assuming uniform distribution. For studies of molecules at low pressures, the mode spacing $\Delta\nu_c$ is in general much larger than the homogeneous linewidth of the absorption transition $\Delta\nu_0$, and the linewidth of each mode is less than $\Delta\nu_0$. Under these conditions the rate of absorption should be given by

$$\gamma_{ab} = \sum_{m=1}^{M} N_1 \sigma_0 \int_{-\infty}^{+\infty} d\nu_a F_m p(\nu_a) g(\nu_a, S_d), \tag{13}$$

with

$$F = \sum_m F_m , \tag{14}$$

$$S_d = 2\tau\sigma_0 (2/\pi\Delta\nu_0) F/M. \tag{15}$$

Here M is the number of modes and F_m is the intensity per mode. With $\Delta\nu_l \gg \Delta\nu_D \gg \Delta\nu_c \gg \Delta\nu_0$, different modes then interact with different regions within the inhomogeneously broadened profile. When the intensity per mode is approximately the same for all modes present, Eq. (13) integrates to

$$\gamma_{ab} \approx N_1 \sigma_0 (F/\Delta\nu_l)(1+S_d)^{-1/2}. \tag{16}$$

Note that when the mode spacing is much less than the homogeneous linewidth, Eq. (11) and (12) should be used instead. For the case with $\Delta\nu_D > \Delta\nu_l \gg \Delta\nu_c \gg \Delta\nu_0$, the rate of absorption is given by

$$\gamma_{ab} \approx N_1 \sigma_0 (F/\Delta\nu_D)(1+S_d)^{-1/2}. \tag{17}$$

B. Application to OH absorption

In the experiments to be discussed in the following sections, both the $P_1(1)$ and $P_1(2)$ lines near 2821.7 and 2825.8 Å, respectively, were used for excitation (see Fig. 1). These absorption lines were chosen for excitation because they originate from highly populated rotational levels in the ground electronic state and because their spectral position could be ascertained experimentally without much interference from neighboring transitions (see Sec. III). For these transitions, the integrated absorption cross section may be given by[7]

$$\sigma_0 = \pi r_0 c f_{01} (\Delta f/f_{01}), \tag{18}$$

where $r_0 = 2.8 \times 10^{-13}$ cm is the classical radius of the electron, c is the speed of light, $f_{01} = 2.3 \times 10^{-4}$ is the band oscillator strength for the $^2\Pi(v''=0) \rightarrow {}^2\Sigma^+(v'=1)$ transitions,[8] and $\Delta f/f_{01}$ is the fraction of the band oscillator strength associated with the particular absorption line used for excitation. Substitution of these numerical values into Eq. (18) gives

$$\sigma_0 = 6.1 \times 10^{-6} \Delta f/f_{01} \text{ cm}^2/\text{sec}. \tag{19}$$

The fraction of the band oscillator strength $\Delta f/f_{01}$, can be deduced from the calculated line transition probabilities for the rotational-electronic transitions involved[9-11] or from the relative intensities in the observed emission spectrum.[9] The results for the $P_1(1)$ and $P_1(2)$ lines are summarized in Table I, along with other transition lines originating from low-lying rotational levels. As is seen from Table I, these two methods give essentially the same results for the fractional oscillator strength of a given transition.

Also included in Table I is the fraction of the molecular concentration, $\Delta n/n$, where n is the OH concentration (molecules/cm^3) in the focal region of excitation, that resides in the particular rotational level from which the absorption transition originates. It follows that

$$N_1 = n(\Delta n/n). \tag{20}$$

The values for $\Delta n/n$ in Table I were computed for the case of a thermalized distribution at a temperature of 300 °K with due regard for the Λ splitting of the rotational levels in the $^2\Pi$ state of OH.

Over the pressure range studied in our experiments, the absorption lines were essentially inhomogeneously broadened with a Doppler width of 0.11 cm^{-1}. This dictates that Eqs. (8), (11), (16), or (17) applies for the results to be discussed below. The corresponding rate of absorption is thus

TABLE I. Normalized oscillator strength $\Delta f/f_{01}$ of the P_1, Q_1, and R_1 transitions of OH determined from calculated rotational transition probabilities and from measured emission-line intensities. The ground-state population distribution $\Delta n/n$ is that for a thermalized distribution at 300 °K.

			$\Delta f/f_{01}$ Normalized oscillator strength		
K''	J''	$\Delta n/n$	$P_1(K'')$	$Q_1(K'')$	$R_1(K'')$
1	$\frac{3}{2}$	0.14	0.59 [a]	0.51 [a]	0.16 [a]
			0.59 [b]	0.56 [b]	0.16 [b]
2	$\frac{5}{2}$	0.14	0.47 [a]	0.67 [a]	0.26 [a]
			0.53 [b]	0.71 [b]	0.25 [b]
3	$\frac{7}{2}$	0.105	0.49 [a]	0.77 [a]	0.32 [a]
			0.52 [b]	0.79 [b]	0.32 [b]
4	$\frac{9}{2}$	0.064	0.50 [a]	0.85 [a]	0.36 [a]
			0.51 [b]	0.84 [b]	0.35 [b]

[a] Deduced from measured emission-line intensities (Ref. 9).

[b] Deduced from calculated rotational transition probabilities (Ref. 10).

given by

$$\gamma_{ab} = 1.8 \times 10^{-15} n(\Delta n/n)(\Delta f/f_{10}) F h(F), \quad (21)$$

where

$$h(F) = [4(\ln 2)/\pi]^{1/2}(1+S_a)^{-1/2}, \quad \Delta\nu_D \gg \Delta\nu_0 \gg \Delta\nu_l, \quad (21a)$$

$$h(F) = (\Delta\nu_D/\Delta\nu_l)(1+S_c)^{-1}, \quad \Delta\nu_l \gg \Delta\nu_D \gg \Delta\nu_0, \quad (21b)$$

$$h(F) = (\Delta\nu_D/\Delta\nu_l)(1+S_d)^{-1/2}, \quad \Delta\nu_l \gg \Delta\nu_D \gg \Delta\nu_c \gg \Delta\nu_0, \quad (21c)$$

$$h(F) = (1+S_d)^{-1/2}, \quad \Delta\nu_D \gg \Delta\nu_l \gg \Delta\nu_c \gg \Delta\nu_0. \quad (21d)$$

C. Spectrum of resonance fluorescence emitted by the excited OH

Over the pressure range (0.1–50 Torr total pressure) studied in our experiments, an appreciable fraction of the excited OH resulting from an absorbing transition will return to the ground electronic state through the emission of a fluorescence photon. The total rate of emission of fluorescence photons, γ_f, is given by

$$\gamma_f = \gamma_{ab}[\gamma/(\gamma+q)], \quad (22)$$

where γ_{ab} is given by Eq. (21), $\gamma \approx 10^6$ sec^{-1} is the radiative emission rate[12] for the excited OH ($^2\Sigma^+$), and q is the rate of quenching of the excited OH ($^2\Sigma^+$) due to other molecular species present in the focal region of excitation. The ratio $\gamma/(\gamma+q)$ determines the fluorescence efficiency.

To determine the fluorescence spectrum, an examination[9] of the Franck-Condon factors for the electronic states involved indicates that fluorescence occurs primarily through the $^2\Sigma^+(v'=1) \rightarrow {}^2\Pi(v''=1)$ and $^2\Sigma^+(v'=0) \rightarrow {}^2\Pi(v''=0)$ transitions with negligible intensities associated with the branches of $^2\Sigma^+(v'=1) \rightarrow {}^2\Pi(v''=0)$ and $^2\Sigma^+(v'=0) \rightarrow {}^2\Pi(v''=1)$ transitions. The relative intensities associated with the former two branches of fluorescence transitions are determined by the extent of rotational and vibrational relaxations that may take place during the lifetime of the OH in the excited state. For the $P_1(1)$ and $P_1(2)$ transition lines used in our experiments, these relaxation processes may take the form of direct vibrational relaxation from $^2\Sigma^+(v'=1)$ to $^2\Sigma^+(v'=0)$ without any change in the rotational energy, or through an exchange of both vibrational and rotational energy of excitation[13] with the total energy of the excited OH remaining essentially unchanged (Fig. 1). With the experiments conducted near ambient temperatures, rotational relaxation within the $^2\Sigma^+(v'=1)$ vibrational manifold will mostly involve the $K'=0$ and $K'=1$ levels only, but may involve all rotational levels with $K' \leq 13$ within the $^2\Sigma^+(v'=0)$ manifold.

Based on the known line transition probabilities[9,10] of OH, one calculates that the fluorescence emitted by a thermalized distribution with the $^2\Sigma^+(v'=1)$ manifold should center around 3145 Å, with the emission primarily associated with the $P_1(1)$, $P_1(2)$, $Q_1(1)$, and $Q_2(1)$ lines; on the other hand, the fluorescence emission should center around 3090 Å if it is from a thermalized distribution within the $^2\Sigma^+(v'=0)$ manifold. The fluorescence spectrum emitted by a nonthermalized distribution involving higher-lying rotational levels can be calculated in a similar manner; the results of such a calculation indicate that the corresponding fluorescence spectrum becomes much more spread out, with the peaks at both 3090 and 3145 Å becoming less pronounced.

It follows from the above discussion that even a low-resolution study of the fluorescence spectrum can yield information on the dominant relaxation process under any given experimental condition. For example, the level $^2\Sigma^+(v'=1, K'=1)$ is within 0.51 cm^{-1} of the level $^2\Sigma^+(v'=0, K'=13)$, whereas no such energy coincidence exists for the $^2\Sigma^+(v'=1, K'=0)$ level.[9] The presence of this energy coincidence would favor a fast cross relaxation between these two groups of levels when $P_1(2)$ is used for excitation. Since the levels $^2\Sigma^+(v'=0, K'=13)$ are associated with higher statistical weight, these are the group of levels where most of the excitation would reside. When this cross relaxation process is predominant, one would thus expect that the fluorescence spectrum excited by $P_1(2)$ should be more concentrated in the $^2\Sigma^+(v'=0) \rightarrow {}^2\Pi(v''=0)$ transition than that excited by $P_1(1)$. On the other hand, the fluorescence spectrum excited by both $P_1(1)$ and $P_1(2)$ lines should be about the same if direct vibrational relaxation is predominant.

The cross relaxation within the excited electronic state discussed above also affects the saturation behavior of the absorption transition through the characteristic relaxation time τ. A similar effect is also to be expected for the cross relaxation within the ground electronic state. However, at the low pressures at which our saturation studies were undertaken, the relaxation time τ is primarily determined by the radiative emission rate γ from the excited state, so that these effects are of negligible importance to a first approximation.

III. EXPERIMENTAL

In our studies of the resonance fluorescence of OH, the tunable radiation near 2825.8 and 2821.7

Å was derived as the second harmonic from the output of a tunable dye laser. The dye laser system consisted of one oscillator and one amplifier, with the oscillator arranged to form a 2-m concentric cavity.[1] This laser system was operated near 5651 and 5643 Å with ultrapurified Rhodamine 6G dissolved in methanol and at a repetition rate of one pulse every 10 sec. To narrow the spectral width of the output, an intracavity Fabray-Perot etalon and a Littrow-mount grating as an end reflector were used. Fine tuning was achieved by varying the mixture of helium and propylene which filled the etalon spacing. The second harmonic was generated in a 5-cm ADP (ammonium dihydrogen phosphate) crystal oriented for index matching. With optimal focusing, an output energy of 0.1 mJ with a pulse duration of 250 nsec and a spectral width of 0.09 cm^{-1} at the second-harmonic frequency was obtained. The exciting radiation was tuned to coincide with the $P_1(1)$ and $P_1(2)$ transitions by observing the enhanced fluorescence near 3090 Å resulting from excitation of the high concentration of OH in a gas burner flame placed at the focal region of excitation. Figure 2 shows the fluorescence signal near 3090 Å as the exciting frequency is tuned around absorption transitions originating from low-lying rotational levels. It is seen from this figure that little interference due to neighboring transitions is involved when $P_1(1)$ or $P_1(2)$ is used for excitation.

For experiments requiring broadband operation, the intracavity Fabray-Perot etalon was removed from the cavity. This resulted in an increase in spectral width to 1.2 cm^{-1} and an increase in energy per pulse to 0.15 mJ with no noticeable change in pulse duration.

Figure 3 shows a schematic of the experimental setup. The second-harmonic beam emerging from the ADP crystal was directed to the center of the OH cell and focused with an 8-cm-focal-length lens to a spot measured to be 2×10^{-4} cm^2 in area. Fluorescence light emanating in a direction 90° from the exciting radiation was collected by an $f/3.6$ collection lens with a focal length of 12.5 cm and imaged with a 50-cm lens into the entrance slit of a spectrometer equipped with a 1200-line/mm grating blazed for 3000 Å. With a slit width of 2 mm, the spectrometer resolution was measured to be a 16 Å and the overall transmission was 40%. The light emerging from the exit slit of the spectrometer was detected by a high-gain RCA 8575 photomultiplier tube and processed by the appropriate photon-counting apparatus.

The experiments were conducted in a Pyrex glass flow system with an inside diameter of 1 cm and a total volume of 0.7 liters. At a pressure

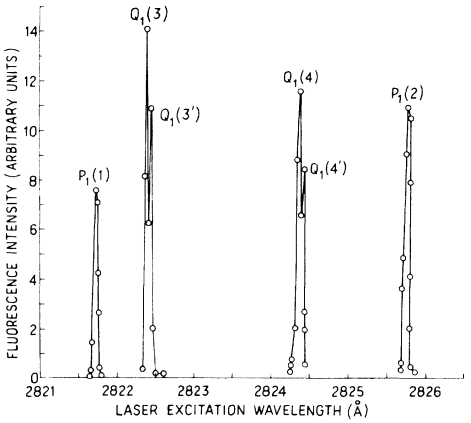

FIG. 2. Fluorescence signal near 3090 Å emitted by OH in a flame as a function of exciting laser frequency.

of 10 Torr of N_2, a flow rate of about 330 cm/sec was measured. The inside of the glassware was coated with 85% phosphoric acid to facilitate free-radical[14] production.

For measurements of intensity dependence, OH was generated through dissociation of water vapor[15] in a 100-W microwave discharge located 30 cm upstream from the focal region of excitation. For other measurements reported in this paper, OH was also generated by first dissociating molecular hydrogen in a microwave discharge followed by reacting the atomic hydrogen[16] thus formed with NO_2 introduced 10 cm upstream from the focal region. Typical concentrations used were 0.1 Torr of water vapor, 0.4 Torr of H_2, and 0.1 Torr of NO_2. In either case, an OH concentration of about 10^{12}–10^{13} molecules/cm^3 was generated.

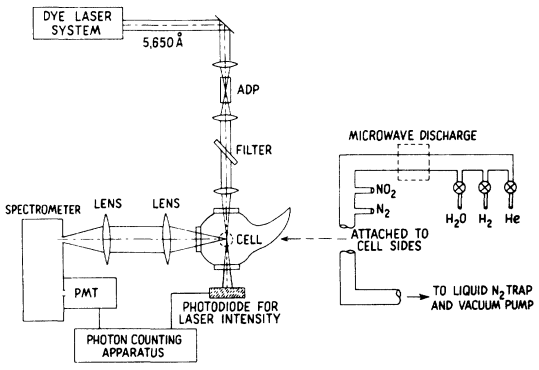

FIG. 3. Schematic of experimental setup.

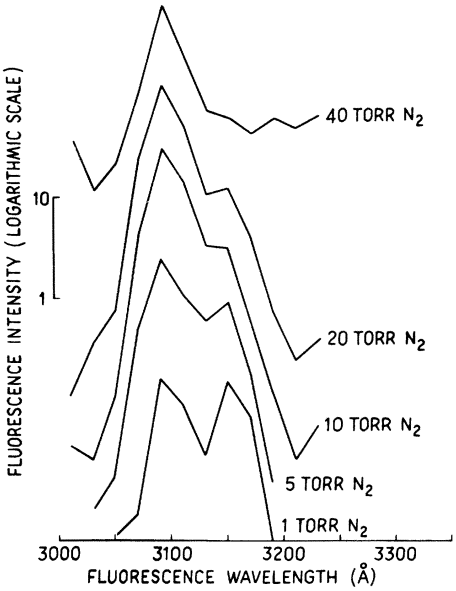

FIG. 4. Composite plot of fluorescence spectrum of OH at different nitrogen pressures with $P_1(1)$ excitation. The data were taken in increments of 20 Å and processed with a spectrometer resolution of 16 Å.

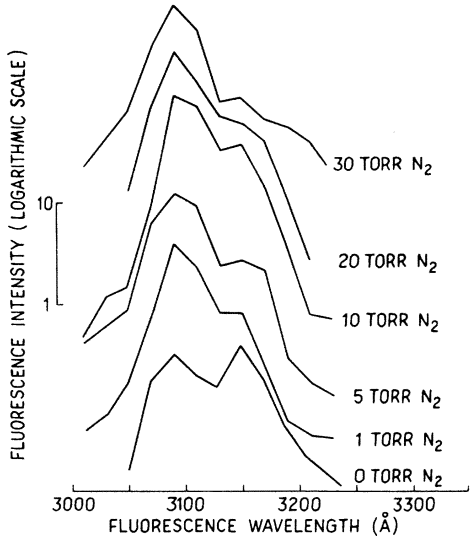

FIG. 5. Composite plot of fluorescence spectrum of OH at different nitrogen pressures with $P_1(2)$ excitation. The data were taken in increments of 20 Å and processed with a spectrometer resolution of 16 Å.

IV. RESULTS AND DISCUSSION

A. Pressure dependence of the fluorescence spectrum of OH

Figure 4 summarizes the pressure dependence of the fluorescence spectrum of OH excited by the $P_1(1)$ transition near 2821.7 Å under nitrogen atmosphere. Similar results obtained with the $P_1(2)$ transition near 2825.8 Å used for excitation are shown in Fig. 5. For the results in both of these figures, the OH was generated through the reaction of NO_2 with atomic hydrogen in a background pressure of 10 Torr of He. Nitrogen was then added into the system downstream from the NO_2 port. Of particular interest in these results are the following observations: (i) There are two peaks in the fluorescence spectrum observed at low pressures, one occuring at 3090 Å and the other at 3145 Å; (ii) there is no detectable shift in the position of the peaks as the pressure is increased; (iii) the ratio of the peak intensity at 3090 Å to that at 3145 Å increases monotonically with the pressure of nitrogen, and at pressures of 40 Torr or higher the fluorescence peaks around 3090 Å only; and (iv) the pressure at which the peak at 3145 Å begins to disappear is much lower (about 1 Torr of N_2) for $P_1(2)$ excitation than that for $P_1(1)$ excitation (about 10 Torr N_2).

The above results can be most readily understood in light of the discussions in Sec. II C. It is to be noted that the location and intensity ratio of the fluorescence peaks should remain the same for both excitations if direct vibrational relaxation is predominant in determining the redistribution of the excited OH, whereas the observed ratio of the peak intensities and the broadening of the peaks would be different for different excitations only if cross (rotational/vibrational) relaxation involving an exchange in both rotational and vibrational energies is also operative. From the lack of any shifts in the position of the observed peaks at all pressures, it follows that there is direct vibrational relaxation of the excited OH owing to species present in the focal region. On the other hand, cross (rotational/vibrational) relaxation involving energy coincidence must also be operative, since the ratio of the peak fluorescence intensities was different for different excitations at low N_2 pressures (≤ 10 Torr) and a slight broadening of the peaks was noted with $P_1(2)$ excitation. However, in order to determine these relaxation rates from the above studies, it would be necessary to determine the fluorescence spectrum with higher resolution, at the expense of greatly reduced signal levels. Our data to date are too crude for such a quantitative determination.

As an attempt to quantify the above conclusions, we have studied the fluorescence spectrum of OH generated as a dissociation produce of 0.1 Torr of water vapor through the microwave discharge. The observed spectrum was similar to those indicated above; however, the ratio of the peak in-

tensity at 3090 Å to that at 3145 Å was found to be the same, 0.44, for both $P_1(1)$ and $P_1(2)$ excitation. These results indicate that direct vibrational relaxation due to water molecules is predominant in determining the redistribution of the excited OH. Taking into account the differences in the radiative emission rate for the $^2\Sigma^+(v'=1) \rightarrow {}^2\Pi(v''=1)$ and $^2\Sigma^+(v'=0) \rightarrow {}^2\Pi(v''=0)$ transitions, one deduces from the observed ratio of the peak intensities that the rate of vibrational relaxation is 0.6×10^6 sec^{-1} for a pressure of 0.1 Torr of water vapor. The rate constant for vibrational relaxation due to water is not known,[13] but it should generally be comparable to, or greater than, the rate constant for electronic quenching.[17,18] This means that the rate of vibrational relaxation due to 0.1 Torr of water vapor should be at least 0.5×10^6 sec^{-1}. Our deduced value of 0.6×10^6 sec^{-1} is in good agreement with this estimate.

B. Intensity dependence of OH fluorescence

In Figs. 6 and 7 the fluorescence signal of OH is shown as a function of the exciting intensity for $P_1(1)$ and $P_1(2)$ excitation, respectively. These results were obtained with the broadband output from the laser used for excitation. Similar results were also obtained when narrowband output was used. It is seen in these figures that the fluorescence signal varies as the square root of the intensity of the exciting radiation within the uncertainty of the measurements, rather than the usually observed linear dependence observed at very low intensities or at high pressures. With the actual OH concentrations used in these experiments, self-trapping of the fluorescence emission is completely negligible, so that the observed deviation from linear dependence must be due to saturation of the absorption transition only.

With the system pressure at 0.1 Torr of H_2O, one calculates the pressure-broadened linewidth[19] for the absorption transition to be $\Delta\nu_0 \approx 0.6\times10^{-4}$ cm^{-1}. This may be compared to the Doppler linewidth of 0.11 cm^{-1}, the cavity mode spacing of 5×10^{-3} cm^{-1} at 2825 Å, and the laser linewidth of 1.2 and 0.09 cm^{-1} for broadband and narrowband operation, respectively. It follows that Eqs. (21c) and (21d) should apply for the case of broadband and narrowband excitation, respectively.

To calculate the saturation parameter according to Eq. (15), one notes that the characteristic relaxation time τ is primarily determined by the rate of the radiative emission and electronic quenching due to water[17,18]; $\tau \approx 0.6\times10^{-6}$ sec with 0.1 Torr of water vapor present. With full laser power incident, one thus obtains from Eq. (15) $S_d \approx 3.4\times10^4$ and $S_d \approx 3\times10^5$ for broadband and narrowband excitation, respectively. This high value of S is consistent with the data in Figs. 6 and 7, where no deviation from the square-root dependence was observed, even down to the lowest laser intensity employed.

At an intensity higher than about 20% of the maximum intensity employed, the power-broadened linewidth $\Delta\nu_0(1+S_d)^{1/2}$ becomes equal to or larger than $\Delta\nu_c$, the spacing between modes of the exciting laser beam. In the limit when the

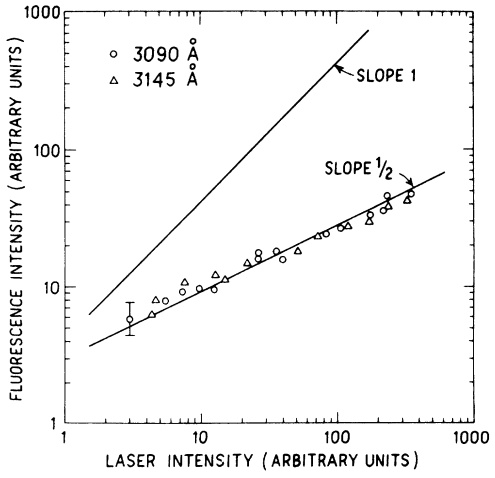

FIG. 6. Fluorescence signal of OH excited by the $P_1(1)$ transition as a function of the intensity of excitation. The relative position of the fluorescence signal near 3090 Å has been multiplied by a factor of $(0.44)^{-1}$, so that the two sets of data coincide.

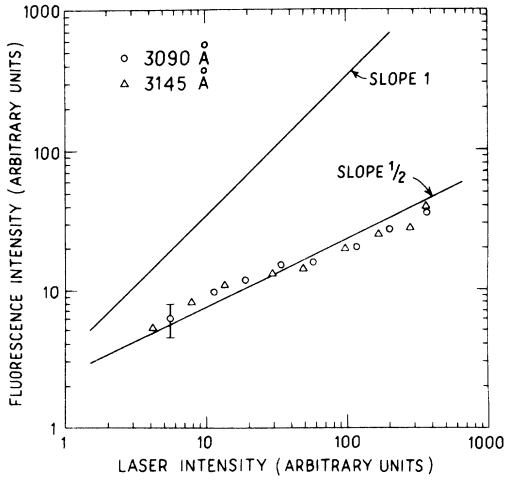

FIG. 7. Fluorescence signal of OH excited by the $P_1(2)$ transition as a function of the intensity of excitation. The relative position of the fluorescence signal near 3090 Å has been multiplied by a factor of $(0.44)^{-1}$, so that the two sets of data coincide.

power-broadened linewidth is greater than the spacing between modes, it is expected that the absorption rate should approach the intensity dependence of Eq. (21b). The systematic deviation observed in Figs. 6 and 7 from the square-root dependence, although within the experimental uncertainty, tends to indicate that such a transition from Eqs. (21c) and (21d) to Eq. (21b) may be occurring.

It is tacitly assumed in the above discussion that the shift of the resonating energy levels due to the quadratic ac Stark effect[20] is negligible. Rough calculation indicates that this effect amounts to a shift of 10^{-1} cm^{-1} or less at the maximum intensity employed in our experiments. This value is much smaller than the linewidth of the exciting laser, and thus is negligible.

The results discussed above demonstrate a good agreement between the predicted and observed intensity dependence for inhomogeneously broadened transitions of OH, and exemplify the importance of laser modes in determining the effective rate of absorption. They should be of interest to studies of other absorption transitions, including the resonant two-photon transitions reported recently,[21,22] and should also be important in the detection of OH at high altitudes in the atmosphere.[4]

ACKNOWLEDGMENTS

It is a pleasure to acknowledge many useful discussions with C. H. Wu and H. Niki regarding the generation of OH in a flow discharge system.

---

*Supported by the Atmospheric Sciences Section, National Science Foundation, through the Department of Physics, University of Michigan, Ann Arbor, Mich.

†Supported in part by NASA Ames Research Center through Contract No. NAS2-8798.

[1]C. C. Wang, Bull. Am. Phys. Soc. 19, 24 (1974); C. C. Wang and L. I. Davis, Jr., Phys. Rev. Lett. 32, 349 (1974).

[2]C. C. Wang and L. I. Davis, Jr., Appl. Phys. Lett. 25, 34 (1974).

[3]R. W. Terhune, private communication.

[4]M. J. Molina and F. W. Rowland, Nature 249, 810 (1974).

[5]R. Karplus and J. Schwinger, Phys. Rev. 73, 1020 (1948).

[6]R. H. Pantell and H. E. Puthoff, *Fundamentals of Quantum Electronics* (Wiley, New York, 1969), pp. 71 and 129.

[7]G. Herzberg, *Spectra of Diatomic Molecules* (Van Nostrand, New York, 1950), p. 383.

[8]P. E. Rouse and R. Engleman, Jr., J. Quant. Spectrosc. Radiat. Transfer 13, 1503 (1973).

[9]G. H. Dieke and H. M. Crosswhite, J. Quant. Spectrosc. Radiat. Transfer 2, 97 (1961).

[10]R. C. M. Learner, Proc. R. Soc. A 269, 311 (1962).

[11]D. M. Golden, F. P. Del Greco, and F. Kaufman, J. Chem. Phys. 39, 3034 (1963).

[12]K. R. German and R. N. Zare, Phys. Rev. Lett. 23, 1207 (1969).

[13]K. H. Welge, S. V. Filseth, and J. Davenport, J. Chem. Phys. 53, 502 (1970).

[14]T. W. Hänsch, S. A. Lee, R. Wallenstein, and C. Wieman, Phys. Rev. Lett. 34, 307 (1975).

[15]R. A. Jones and C. A. Winkler, Can. J. Chem. 29, 1010 (1951).

[16]J. G. Anderson, J. J. Margitan, and F. Kaufman, J. Chem. Phys. 60, 3310 (1974).

[17]D. Kley and K. H. Welge, J. Chem. Phys. 49, 2870 (1968).

[18]K. H. Becker and D. Haaks, Z. Naturforsch. A 28, 249 (1973).

[19]R. Engleman, Jr., J. Quant. Spectrosc. Radiat. Transfer 9, 391 (1969).

[20]P. F. Liao and J. E. Bjorkholm, Phys. Rev. Lett. 34, 1 (1975).

[21]C. C. Wang and L. I. Davis, Jr., Phys. Rev. Lett. 35, 650 (1975).

[22]J. F. Ward and A. V. Smith, Phys. Rev. Lett. 35, 653 (1975).